

Sparse Bayesian Causal Forests for Heterogeneous Treatment Effects Estimation

Alberto Caron *

Department of Statistical Science
University College London

Gianluca Baio

Department of Statistical Science
University College London

Ioanna Manolopoulou

Department of Statistical Science
University College London

December 23, 2024

Abstract

This paper develops a sparsity-inducing version of Bayesian Causal Forests, a recently proposed nonparametric causal regression model that employs Bayesian Additive Regression Trees and is specifically designed to estimate heterogeneous treatment effects using observational data. The sparsity-inducing component we introduce is motivated by empirical studies where the number of pre-treatment covariates available is non-negligible, leading to different degrees of sparsity underlying the surfaces of interest in the estimation of individual treatment effects. The extended version presented in this work, which we name Sparse Bayesian Causal Forest, is equipped with an additional pair of priors allowing the model to adjust the weight of each covariate through the corresponding number of splits in the tree ensemble. These priors improve the model's adaptability to sparse settings and allow to perform fully Bayesian variable selection in a framework for treatment effects estimation, and thus to uncover the moderating factors driving heterogeneity. In addition, the method allows prior knowledge about the relevant confounding pre-treatment covariates and the relative magnitude of their impact on the outcome to be incorporated in the model. We illustrate the performance of our method in simulated studies, in comparison to Bayesian Causal Forest and other state-of-the-art models, to demonstrate how it scales up with an increasing number of covariates and how it handles strongly confounded scenarios. Finally, we also provide an example of application using real-world data.

*This work was supported by a British Heart Foundation-Turing Cardiovascular Data Science Award (BCDSA/100003). Corresponding author: alberto.caron.19@ucl.ac.uk, 1-19 Torrington Pl, London WC1E 7HB.

1 Introduction

Inferring the effect of a treatment at an individual level in a population of interest lies at the heart of disciplines such as precision medicine or personalized advertisement, where decision making for treatment administration is based on the characteristics of each single unit of analysis. The ever-increasing amount of observational data readily available offers a unique opportunity for drawing inferences at the resolution of each individual. However, since Individual Treatment Effects (ITEs) are never directly observable in the real world, standard supervised learning techniques cannot be directly applied. Moreover, the process of treatment allocation in large, observational datasets is usually unknown and can obscure the effect of the actual treatment through confounding (Dawid, 2000; Pearl, 2009a; Imbens and Rubin, 2015).

The application of statistical learning tools for causal inference has led to significant improvements in the estimation of heterogeneous treatment effects. These improvements stem from the predictive power of advanced nonparametric regression models, that, after being appropriately adapted to the causal inference setting, can leverage large observational datasets and capture non-linear relationships. Caron et al. (2020) provide a review of the most recent popular methods, together with a comparison of their performance.

Two of the early contributions that paved the way towards the use of tree-based statistical learning tools on large datasets for causal analysis purposes are Foster et al. (2011) and Hill (2011), who advocate the use of tree ensemble methods for the estimation of ITE. The former focuses on randomized experiments (randomized control trials) and makes use of Random Forests (Breiman, 2001); the latter instead addresses the problem from an observational study perspective, and employs Bayesian Additive Regression Trees (BART) (Chipman et al., 1998, 2010). Another popular tree-based method is Causal Forests (CF), developed by Wager and Athey (2018), where the authors develop a causal version of Random Forests. Recently, Hahn et al. (2020) build on the work of Chipman et al. (2010) and Hill (2011) to formulate a different BART framework, under the name of Bayesian Causal Forests (BCF), specifically designed to address strong confounding and capture prognostic and moderating effects of the covariates when estimating ITE. Here, the prognostic effect (or prognostic score) is defined as the impact of the covariates on the outcome in the absence of treatment, while the moderating effect is the impact of the covariates on treatment effect, namely what causes treatment effects to be heterogeneous across individuals.

A different stream of contributions that do not focus on any specific regression model is that of *Meta-Learners*. Meta-Learners are meta-algorithms that design a procedure to estimate ITE via any suitable regression model for supervised prediction (e.g. LASSO regression, random forests, BART, neural networks), without the need of adjusting existing structure of the model. Recent popular work on Meta-Learners include Künzel et al. (2017), where the authors develop a framework to deal with unbalanced treatment groups (named X-Learner), and Nie and Wager (2020), where parametrization in Robinson (1988) is exploited (hence the name R-Learner) to design a loss function for parameter tuning on ITE. Among other notable works on heterogeneous treatment effects estimation, Alaa and van der Schaar (2017, 2018)

adopt a multi-task learning approach to ITE estimation using Gaussian Processes, while Johansson et al. (2016), Shalit et al. (2017) and Yao et al. (2018) employ deep neural networks to learn balanced representations that aim at minimizing the distributional distance between treatment groups.

The aforementioned contributions typically rely on a large number of observations to learn treatment effects. However, large observational datasets often come with a very large number of pre-treatment covariates too, many of which may not directly affect the treatment effect or the response variable in question. Hence, complexity of ITE estimation inevitably depends on the smoothness and sparsity of the surfaces of interest (Alaa and van der Schaar, 2018), and necessitates regularization. At the same time, prior subject-matter knowledge on the relative importance of the covariates may be available, and can improve estimates if embedded in the model. In light of these considerations, none of the above mentioned nonparametric approaches allow to jointly: i) account for heterogeneous smoothness and sparsity across covariates; ii) tease apart prognostic and moderating covariates through targeted variable selection; iii) incorporate prior knowledge on the relevant covariates and their relative impact on the outcome. Carefully designed regularization can lead to improved ITE estimates and inferences of prognostic and moderating factors, since including a large number of pre-treatment covariates in a fully-saturated model to adjust for confounding may lead to misspecification. To this end, we propose an extension of the Bayesian Causal Forest framework (Hahn et al., 2020), consisting of additional Dirichlet prior distributions as in Linero (2018), to implement fully Bayesian variable selection and to reflect prior knowledge on the relative importance of different covariates driving the prognostic and moderating effects respectively. BART (and consequently BCF) was originally designed to adapt to smoothness but not to sparsity¹. Our extended version of the model can be easily fitted with a slight modification of the existing backfitting MCMC algorithm and results in improved ITE estimates and better adaptation to sparsity, which induces different levels of smoothness across covariates. We demonstrate improved performance of our model also in cases where the number of covariates P is way smaller than sample size N ($P \ll N$), at negligible extra computational cost.

The rest of the paper is organized as follows. Section 2 introduces the problem of estimating treatment effects using the Neyman-Rubin causal model framework, and since we adopt the perspective of an observational study, it also formulates the necessary assumptions to recover treatment effect estimates under confounding. Section 3 offers an overview on Bayesian Additive Regression Trees and their popular causal version, Bayesian Causal Forest. Section 4 introduces our sparse extension, under the name of “Sparse Bayesian Causal Forest”. Section 5 presents results from simulated studies carried out to compare Sparse Bayesian Causal Forest performance with other state-of-the-art models. Section 6 provides an example of analysis using data from the Infant Health and Development Program aimed at investigating the effects of early educational support on cognitive abilities in low birth weight infants. Section

¹Regularization in BART is introduced via shallow trees structures, to avoid overfitting (similarly to Gradient Boosting). Linero and Yang (2018) propose a way to further enhance smoothness adaptation in BART through a probabilistic version of the trees, where inputs follow a probabilistic, rather than deterministic, path to the terminal nodes.

7 concludes with a discussion.

2 Problem framework

In this section we outline the problem of deriving an estimator for the quantity of interest, known as *Conditional Average Treatment Effect* (CATE), through observed quantities (identification). We follow the Neyman-Rubin potential outcomes framework, as described in Rubin (1978) and Imbens and Rubin (2015) among others, where causal inference is represented as a missing data problem². We consider a setup where the outcome variable is continuous and the treatment assignment is binary (of the type exposure versus non-exposure), but the notions and concepts of this section can be potentially generalized to non-continuous responses and more than two treatment arms. For each individual $i \in \{1, \dots, N\}$, the two potential outcomes are defined as $Y_i^{(Z_i)}$, where $Z_i \in \{0, 1\}$ is the binary treatment assignment, with $Z_i = 1$ indicating exposure to the treatment, while $Z_i = 0$ non-exposure. We consider throughout this work continuous type of outcomes, such that $(Y_i^{(0)}, Y_i^{(1)}) \in \mathbb{R}^2$. Given the potential outcomes and the binary treatment assignment, ITE is defined, for each individual i , as the difference $Y_i^{(1)} - Y_i^{(0)}$. The fundamental problem of causal inference is that, for each i , we get to observe only one of the two potential outcomes $(Y_i^{(0)}, Y_i^{(1)}) \in \mathbb{R}^2$, specifically the one corresponding to the realization of Z_i , i.e. $Y_i = Z_i Y_i^{(1)} + (1 - Z_i) Y_i^{(0)}$, so that ITE is never observable.

Given a dataset $\{\mathbf{X}_i, Z_i, Y_i\}$ of sample size N , where $\mathbf{X}_i \in \mathcal{X}$ are P pre-treatment covariates, the goal is to derive an estimate of CATE, defined as

$$\tau(\mathbf{x}_i) = \mathbb{E}\left[Y_i^{(1)} - Y_i^{(0)} \mid \mathbf{X}_i = \mathbf{x}_i\right]. \quad (1)$$

In order to estimate $\tau(\mathbf{x}_i)$ through the observed quantities $\{\mathbf{X}_i, Z_i, Y_i\}$, a common set of assumptions are necessary to achieve identification. First of all, we assume that *Stable Unit Treatment Value Assumption* (SUTVA) holds, ensuring that one unit's outcome is not affected by other units' assignment to treatment. The second assumption is unconfoundedness, expressed through the conditional independence $(Y_i^{(0)}, Y_i^{(1)}) \perp\!\!\!\perp Z_i \mid \mathbf{X}_i$, and ensures that there are no unobserved covariates simultaneously affecting selection into treatment and outcome (no unobserved confounders). The third and final assumption is common support, which means that all units have a probability of falling into either treatment groups which is strictly between 0 and 1. More formally, after defining the propensity score as the probability of unit i being selected into treatment given \mathbf{x}_i ,

$$\pi(\mathbf{x}_i) = \mathbb{P}(Z_i = 1 \mid \mathbf{X}_i = \mathbf{x}_i), \quad (2)$$

common support implies $\pi(\mathbf{x}_i) \in (0, 1) \ \forall i \in \{1, \dots, N\}$, so that there is no deterministic assignment to one of the groups given features $\mathbf{X}_i = \mathbf{x}_i$. Note that unconfoundedness and

²Note that identification of the quantity of interest (CATE) can be achieved also with other causal frameworks, such as *do*-calculus in Structural Causal Models (Pearl, 2009a), or decision-theoretic approach (Dawid, 2000, 2015), and the contribution of this work, which concerns solely estimation, still apply.

common support are automatically satisfied in the case of fully randomized experiments. While the degree of overlap between the two treatment groups can be typically examined in the data, SUTVA and unconfoundedness are untestable assumptions, and their plausibility must be justified based on domain knowledge.

In this work, we focus on non-parametric regression-based approaches to CATE estimation. Imbens (2004) offers a comprehensive overview on different methodologies (regression-based, matching-based, etc.) to estimate individual and population level causal effects. A non-parametric regression approach entails modelling the response surface Y as an unknown function of the covariates and treatment assignment indicator, and an error term. As typically done in the vast majority of the contributions on regression-based CATE estimation, we assume that the error term is additive and normally distributed with zero mean, such that Y_i is modelled as

$$Y_i = f(\mathbf{X}_i, Z_i) + \varepsilon_i, \quad \text{where } \varepsilon_i \sim \mathcal{N}(0, \sigma^2) \quad (3)$$

and where $f(\cdot)$ is of unknown form, and learnt from the data. A broad variety of methods to retrieve a CATE estimator from equation (3) have been developed in the literature (see Caron et al. (2020) for a review and comparison of the most popular ones). Among these, we will follow in particular the one presented in Hahn et al. (2020), that we introduce and discuss in the next section.

3 BART for causal inference

Bayesian Additive Regression Trees (BART) are a non-parametric regression model that estimates the conditional expectation of a response variable Y_i via a “sum-of-trees”. Considering the regression framework in (3), one can use BART to flexibly represent $f(\cdot)$ as:

$$f(\mathbf{X}, Z) = \sum_{j=1}^m g_j([\mathbf{X} \ Z], (T_j, M_j)), \quad (4)$$

where m is the total number of trees in the model; the pair (T_j, M_j) defines the structure of the j -th tree, namely T_j embeds the collection of binary split rules while $M_j = \{\psi_1, \dots, \psi_b\}$ the collection of b terminal nodes in that tree; $g_j(\cdot)$ is a tree-specific function mapping the predictors $[\mathbf{X} \ Z]$ to the set of terminal nodes M_j , following the set of binary split rules expressed by T_j . The conditional mean function $f(\mathbf{x}, z) = \mathbb{E}[Y_i \mid \mathbf{X}_i = \mathbf{x}_i, Z_i = z_i]$ fit is computed by summing up all the terminal nodes ψ_{ij} assigned to the predictors $[\mathbf{X} \ Z]$ by the tree functions $g_j(\cdot)$, i.e. $\sum_{j=1}^m g_j(\cdot)$. All the details about BART prior specification and inference can be found in Chipman et al. (1998) and Chipman et al. (2010).

3.1 Bayesian Causal Forests

As briefly mentioned in Section 2, we will follow the representation proposed by Hahn et al. (2020), that avoids imposing direct regularization on $f(\cdot)$ in (3). Hahn et al. (2018) and Hahn et al. (2020) in fact show that regularization on $f(\cdot)$ can generate unintended bias in

the final estimation of CATE, and propose a simple reparametrization of (3) that utilizes a two-stage regression approach that dates back to the early contribution of Heckman (1979). The two-stage representation reads:

$$Z_i \sim \text{Bernoulli}(\pi(\tilde{\mathbf{X}}_i)) , \quad \pi(\tilde{\mathbf{x}}_i) = \mathbb{P}(Z_i = 1 \mid \tilde{\mathbf{X}}_i = \tilde{\mathbf{x}}_i) , \quad (5)$$

$$Y_i = \mu\left(\begin{bmatrix} \mathbf{X}_i & \pi(\tilde{\mathbf{X}}_i) \end{bmatrix}\right) + \tau(\mathbf{W}_i)Z_i + \varepsilon_i . \quad (6)$$

The first stage (5) deals with propensity score estimation, for which any probabilistic classifier is suitable (e.g. logistic regression, Probit BART, neural nets, etc.). Note that the regressors in the propensity score model are denoted by $\tilde{\mathbf{X}}_i \in \mathcal{X}$ to indicate that a subset of covariates different to \mathbf{X}_i can be employed. The second stage (6) estimates the prognostic score $\mu(\cdot)$, defined as the effect of the covariates $\mathbf{X}_i \in \mathcal{X}$ on the outcome Y_i in the absence of treatment $\mu(\mathbf{x}_i) = \mathbb{E}[Y_i \mid \mathbf{X}_i = \mathbf{x}_i, Z_i = 0]$, and CATE $\tau(\cdot)$. Notice that \mathbf{W}_i appears instead of \mathbf{X}_i in the $\tau(\cdot)$ function, to highlight the fact that, as in the propensity score model, a different set of covariates may be used for CATE estimation. The two-stage procedure described above belongs to a class of models known as “modularized”, as opposed to full-model approaches that attempt to embed uncertainty around propensity scores in a single stage, which can lead to poor estimates due to feedback issues in the approximation of the full posterior (Zigler et al., 2013; Zigler and Dominici, 2014). See Jacob et al. (2017) for a thorough discussion on the issue of modularized versus full/joint models.

A Bayesian Causal Forest model (Hahn et al., 2020) is based on the reparameterization of the second stage regression (6). The advantage of this reparametrization from a Bayesian standpoint lies in the fact that separate priors can be placed on the prognostic score $\mu(\cdot)$ and on CATE $\tau(\cdot)$ directly. This approach mitigates unintended bias attributable to what the authors call *Regularization Induced Confounding* (RIC). The intuition behind RIC is that CATE posterior is strongly influenced by the regularization effects of the prior on $f(\cdot)$ in (3), such that posterior estimates of CATE are bound to be biased, even more so in presence of strong confounding, such as when treatment selection is suspected to be “targeted”, i.e., when individuals are selected into treatment based on the prediction of an adverse potential outcome if left untreated. In order to alleviate confounding from targeted selection, the authors suggest to employ propensity score estimates obtained from the first stage $\hat{\pi}$ as an additional covariate in the estimation of $\mu(\cdot)$.

In practice, a BCF model assigns a default BART prior to $\mu(\cdot)$, while a prior with stronger regularization is chosen for $\tau(\cdot)$, as moderating patterns are believed to be simpler. The BART prior on $\tau(\cdot)$, compared to the default specification, consists in the use of a smaller number of trees in the ensemble (50 trees instead of 200), and a different combination of hyperparameters that govern the depth of each tree, namely $(\nu, \beta) = (0.25, 3)$ instead of the default $(\nu, \beta) = (0.95, 2)$, with the purpose of assigning higher probability mass to smaller trees. This combination of hyperparameters in the CATE prior allows to detect weak heterogeneous patterns, and provides robustness in case of homogeneous treatment effects.

For the reasons illustrated above, BCF tends to outperform BART and other tree-based

methods for CATE estimation, such as Causal Forests (Wager and Athey, 2018). As we will illustrate in the following sections, our work extends the BCF framework to accommodate sparse solutions and thus induce different levels of smoothness across covariates, while allowing, at the same time, to perform variable selection separately on $\mu(\cdot)$ and $\tau(\cdot)$, as well as incorporate prior domain knowledge about the relevant covariates and the magnitude of their impact on the outcome.

4 Sparse Bayesian Causal Forests

BART, and consequently BCF, are known to handle sparsity quite well, thanks to the fact that splitting variables are chosen uniformly at random. However, they do not actively implement heterogeneous sparsity, nor variable selection, which implies assigning equal level of heterogeneity to every covariate included in the model. We will briefly illustrate in this section the notion of variable selection in the context of tree ensemble models such as BART. Let us define first $\mathbf{s} = (s_1, \dots, s_P)$ as the vector of splitting probabilities of each predictor $j \in \{1, \dots, P\}$, where each s_j represents the probability, for the j -th predictor, of being chosen as a splitting variable in one of the decision nodes of a tree. The default version of BART places a uniform distribution over the splitting variables, meaning that each predictor has equal chance of being picked as a splitting variable: $s_j = P^{-1} \quad \forall j \in \{1, \dots, P\}$. As a consequence, predictors are virtually given equal importance in the fit. A sparsity-inducing solution in this framework implies having a vector \mathbf{s} of “stick-breaking” posterior splitting probabilities where ideally the entries corresponding to irrelevant predictors are very close to zero, while the ones corresponding to relevant predictors are significantly higher than P^{-1} . Posterior splitting probabilities in this context can be intuitively viewed as a measure of variables importance (Breiman, 2001). A complementary, decision-theoretic interpretation of sparsity-inducing solutions in this setup is given by the posterior probabilities that a predictor j appears in a decision node at least once in the ensemble. The two interpretations above (variables importance and probability of inclusion) are interchangeable and qualitatively lead to the same conclusions. In the next section we review how the sparse extension of BART proposed by Linero (2018) can accommodate sparse solutions as described above, and how this modified version of BART can be put to use in the context of Bayesian Causal Forests.

4.1 Dirichlet Additive Regression Trees

Dirichlet Additive Regression Trees (Linero, 2018) constitute an effective and practical way of inducing sparsity in BART. The modification consists in placing an additional Dirichlet prior on the vector of splitting probabilities \mathbf{s} , which triggers a consequent posterior update in the backfitting MCMC algorithm. The Dirichlet prior on \mathbf{s} reads

$$(s_1, \dots, s_P) \sim \text{Dirichlet} \left(\frac{\alpha}{P}, \dots, \frac{\alpha}{P} \right), \quad (7)$$

where α is the hyperparameter governing the a priori preference for sparsity. Lower values of α correspond to sparser solutions, that is, fewer predictors included in the model. The hyperparameter α is in turn assigned a prior distribution, in order to deal with unknown degree of sparsity. This prior is chosen to be a Beta distribution, placed over a standardized version of the α parameter, of the following form

$$\frac{\alpha}{\alpha + \rho} \sim \text{Beta}(a, b) , \quad (8)$$

where the default parameter values are $(a, b, \rho) = (0.5, 1, P)$. The combination of values $a = 0.5$ and $b = 1$ assigns higher probability to low values of α , thus giving preference to sparse solutions (the combination $(a, b) = (1, 1)$ would instead revert back to default BART splitting probabilities, i.e. uniform distribution over the splitting variables). The prior is assigned to the standardized version of α in (8) instead of α directly, as this allows to easily govern preference for sparsity through the parameter ρ . If one suspects that the level of sparsity is, although unknown, rather high, setting a smaller value of ρ facilitates even sparser solutions.

Linero (2018) modifies BART Gibbs sampler to include the update on \mathbf{s} . The modification implies an extra step according to the posterior probability

$$s_1, \dots, s_P \mid (u_1, \dots, u_P) \sim \text{Dirichlet} \left(\frac{\alpha}{P} + u_1, \dots, \frac{\alpha}{P} + u_P \right) , \quad (9)$$

where the update depends on u_j , defined as the number of attempted splits on the j -th predictor in the current MCMC iteration. The phrase “attempted splits” refers to the fact that BART MCMC algorithm generates trees through a branching process undergoing a Metropolis-Hastings step, so that a proposed tree in the process might be rejected, but the chosen splitting variables are counted anyway in $\mathbf{u} = (u_1, \dots, u_P)$. Details on BART MCMC algorithm can be found in Chipman et al. (1998), Chipman et al. (2010) and Linero and Yang (2018).

The rationale behind the update in (9) follows the natural Dirichlet-Multinomial conjugacy. The more frequently a variable is chosen for a splitting rule in the trees of the ensemble in a given MCMC iteration (or equivalently the higher is u_j), the higher the weight given to that variable by the updated $\mathbf{s} \mid (u_1, \dots, u_P)$ in the next MCMC iteration. Hence, the higher s_j , the higher the chance for the j -th predictor of being drawn as splitting variable from the multinomial distribution described by $\text{Multinom}(1, \mathbf{s} \mid \mathbf{u})$. This extra Gibbs step comes at negligible computational cost, when compared to default BART typical running time.

4.2 Sparse BCF priors

Similarly to Linero (2018), symmetric Dirichlet priors can be straightforwardly embedded in the Bayesian Causal Forest framework to induce sparse estimation of prognostic and moderating effects. Bearing in mind that, as described in the previous section, BCF prior consists in two different sets of independent BART priors, respectively placed on the prognostic score $\mu(\cdot)$ and CATE $\tau(\cdot)$, our proposed extension implies adding an additional Dirichlet prior over

the splitting probabilities to these BART priors. Throughout the rest of the work we will consider the case where $\mathbf{W}_i = \mathbf{X}_i$, i.e. where the same set of covariates is used for the estimation of $\mu(\cdot)$ and $\tau(\cdot)$ (see eq. (6) for reference), but the ideas easily extend to scenarios where a different set of covariates is designed, based on domain knowledge, to be used for $\mu(\cdot)$ and $\tau(\cdot)$ ³. The additional priors are respectively

$$\begin{aligned} \mathbf{s}_\mu &\sim \text{Dirichlet} \left(\frac{\alpha_\mu}{P+1}, \dots, \frac{\alpha_\mu}{P+1} \right) , & \frac{\alpha_\mu}{\alpha_\mu + \rho_\mu} &\sim \text{Beta}(a, b) \\ \mathbf{s}_\tau &\sim \text{Dirichlet} \left(\frac{\alpha_\tau}{P}, \dots, \frac{\alpha_\tau}{P} \right) , & \frac{\alpha_\tau}{\alpha_\tau + \rho_\tau} &\sim \text{Beta}(a, b) , \end{aligned} \quad (10)$$

where the Beta parameters are chosen to be $(a, b) = (.5, 1)$ as default. The hyperparameter ρ is set equal to $(P+1)$ in the case of the prognostic score ($\rho_\mu = P+1$) since, when estimating $\mu(\mathbf{x}_i)$, we make use of P covariates plus an estimate of the propensity score $\widehat{\pi}(\mathbf{x}_i)$ as an additional covariate. In the case of $\tau(\mathbf{x}_i)$, we set it equal to $\rho_\tau = \frac{P}{2}$ to give preference to even sparser solutions, as the CATE is typically believed to display simple heterogeneity patterns and a higher degree of sparsity compared to the prognostic score.

We refer to this setup as Sparse Bayesian Causal Forest (Sparse BCF). Naturally, the two Dirichlet priors trigger two separate extra steps in the Gibbs sampler, implementing draws from the posterior Dirichlet distributions:

$$\begin{aligned} \mathbf{s}_\mu \mid \mathbf{u}_\mu &\sim \text{Dirichlet} \left(\alpha_\mu/(P+1) + u_{1\mu}, \dots, \alpha_\mu/(P+1) + u_{(P+1)\mu} \right) \\ \mathbf{s}_\tau \mid \mathbf{u}_\tau &\sim \text{Dirichlet} \left(\alpha_\tau/P + u_{1\tau}, \dots, \alpha_\tau/P + u_{P\tau} \right) . \end{aligned} \quad (11)$$

Sparse BCF setup allows first of all to adjust the model to different degrees of sparsity in $\mu(\cdot)$ and $\tau(\cdot)$, and thus to induce different levels of smoothness across the covariates. Secondly, it naturally implements variable selection on both the prognostic score and CATE separately, given that separate draws of the posterior splitting probabilities are returned. The extra computational cost, in terms of running time, is negligible compared to default BCF. A sketch of pseudo-code illustrating the backfitting MCMC algorithm in Sparse BCF can be found in Box 1.

The Dirichlet priors in Sparse BCF can be also adjusted to convey priori information about the relevant covariates and their relative impact on the outcome. This is of interest in case one would like to incorporate subject-matter knowledge. This can be achieved by introducing a set of prior weights $\mathbf{k} = \{k_1, \dots, k_P\} \in \mathbb{R}_+^P$ in the Dirichlet priors, such that

$$\begin{aligned} \mathbf{s}_\mu &\sim \text{Dirichlet} \left(k_{1\mu} \cdot \frac{\alpha_\mu}{P+1}, \dots, k_{(P+1)\mu} \cdot \frac{\alpha_\mu}{P+1} \right) , \\ \mathbf{s}_\tau &\sim \text{Dirichlet} \left(k_{1\tau} \cdot \frac{\alpha_\tau}{P}, \dots, k_{P\tau} \cdot \frac{\alpha_\tau}{P} \right) . \end{aligned} \quad (12)$$

³In certain cases, the set of pre-treatment covariates might benefit from an initial screening by the researcher in the design of the study, and later undergo the variable selection process in Sparse BCF, with the possibility of incorporating further a priori knowledge through the prior distributions, as described later in this section. As we will show in Section 4.3, in fact, Sparse BCF not only implements sparse solutions per se, but allocates splitting probabilities in a more efficient way among the covariates, compared to uniformly at random splits.

Algorithm 1: Bayesian Backfitting MCMC in Sparse BCF

Input: Data (X, Z, Y)

Output: MCMC samples of $\{\mu^{(b)}(\cdot), \tau^{(b)}(\cdot), (\mathbf{s}_\mu | \mathbf{u}_\mu)^{(b)}, (\mathbf{s}_\tau | \mathbf{u}_\tau)^{(b)}, \sigma^{(b)}\}_{b=1}^B$

for $b = 1, \dots, B$ **do**

Result: Sample $\mu^{(b)}(\mathbf{x}), (\mathbf{s}_\mu | \mathbf{u}_\mu)^{(b)}$

for $j = 1, \dots, m_\mu$ **do**

Sample tree structure $T_j \mu \sim p(T_j | R_j, \sigma) \propto p(T_j) p(R_j | T_j, \sigma)$

Sample terminal nodes $M_j \mu \sim p(M_j | T_j, R_j, \sigma)$ (conjugate normal)

end

Sample $(\mathbf{s}_\mu | \mathbf{u}_\mu) \sim \mathcal{D}(\alpha_\mu/(P+1) + u_{1\mu}, \dots, \alpha_\mu/(P+1) + u_{(P+1)\mu})$

Result: Sample $\tau^{(b)}(\mathbf{x}), (\mathbf{s}_\tau | \mathbf{u}_\tau)^{(b)}$

for $j = 1, \dots, m_\tau$ **do**

Sample tree structure $T_j \tau \sim p(T_j | R_j, \sigma) \propto p(T_j) p(R_j | T_j, \sigma)$

Sample terminal nodes $M_j \tau \sim p(M_j | T_j, R_j, \sigma)$ (conjugate normal)

end

Sample $(\mathbf{s}_\tau | \mathbf{u}_\tau) \sim \mathcal{D}(\alpha_\tau/P + u_{1\tau}, \dots, \alpha_\tau/P + u_{P\tau})$

Result: Sample $\sigma^{(b)}$

Sample $\sigma \sim p(\sigma | \hat{\mu}(\mathbf{x}_i), \hat{\tau}(\mathbf{x}_i), Y)$

end

The weights can take on different values for each covariate and can be set separately for prognostic score and CATE. If the j -th covariate is believed to be significant in predicting $\mu(\cdot)$, then its corresponding prior weight $k_{j\mu}$ can be set higher than the others, in order to generate draws from a Dirichlet distribution that allocate higher splitting probability to that covariate. In the simulated experiment of Section 5.2 we will introduce a version of Sparse BCF with informative priors assigning higher a priori weight to the propensity score in $\mu(\mathbf{x}_i, \pi(\mathbf{x}_i))$, to investigate whether this helps tackling strong confounding.

4.3 Targeted sparsity and covariate heterogeneity

As a result of a fully Bayesian approach to variable selection, Sparse BCF returns non-uniform posterior splitting probabilities that assign higher weight to more predictive covariates. This automatically translates into more splits along covariates with higher predictive power, whereas the default BCF uniform distribution will, on average, allocate the same number of splits across them. To investigate whether this more strategic allocation of splitting probabilities in Sparse BCF leads to better performance, we test it against a default version of BCF including all the covariates and a version of BCF that already employs the subset of relevant covariates only. Think of the latter as a sort of “oracle” BCF that knows, a priori, the subset of relevant covariates, but may not assign different weights to them in terms of relative importance in the estimation of $\mu(\cdot)$ and $\tau(\cdot)$ respectively. To better illustrate the concept,

Table 1: Sample average bias, $\sqrt{\text{PEHE}}$ and 95% coverage for default BCF, “oracle” BCF using the 5 relevant predictors (Oracle BCF-5) and Sparse BCF (SP-BCF). Bold text represents better performance.

Model	Bias	$\sqrt{\text{PEHE}}$	95% Coverage
BCF	0.037 ± 0.008	0.447 ± 0.006	0.92 ± 0.01
Oracle BCF-5	0.034 ± 0.008	0.440 ± 0.006	0.91 ± 0.01
SP-BCF	0.031 ± 0.007	0.380 ± 0.006	0.88 ± 0.01

we run a simple simulated example with $P = 10$ correlated covariates, of which only 5 are relevant, meaning that they exert some effect on the prognostic score or on CATE. We compare default BCF, “oracle” BCF using the 5 relevant covariates only and Sparse BCF using all the covariates (5 relevant and 5 nuisance). We generate the $P = 10$ covariates from a multivariate Gaussian $(X_1, \dots, X_{10}) \sim \mathcal{N}(\mathbf{0}, \Sigma)$, where the entries of the covariance matrix are such that $\Sigma_{jk} = 0.6^{|j-k|} + 0.1\mathbb{I}(j \neq k)$, indicating positive correlation between predictors. Sample size is set equal to $N = 1000$. We then generate treatment assignment as $Z_i \sim \text{Bern}(\pi(\mathbf{x}_i))$, where the propensity score is

$$\pi(\mathbf{x}_i) = \mathbb{P}(Z_i = 1 \mid \mathbf{X}_i = \mathbf{x}_i) = \Phi(-0.4 + 0.3X_{i,1} + 0.2X_{i,2}) . \quad (13)$$

The prognostic score, CATE and response Y_i are respectively generated as

$$\begin{aligned} \mu(\mathbf{X}_i) &= 3 + X_{i,1} + 0.8 \sin(X_{i,2}) + 0.7X_{i,3}X_{i,4} - X_{i,5} , \\ \tau(\mathbf{X}_i) &= 2 + 0.8X_{i,1} - 0.3X_{i,12}^2 , \\ Y_i &= \mu(\mathbf{x}_i) + \tau(\mathbf{x}_i)Z_i + \varepsilon_i , \quad \text{where } \varepsilon_i \sim \mathcal{N}(0, 1) . \end{aligned} \quad (14)$$

In this experiment only the first five predictors are relevant. Table 1 shows performances of the default BCF, “oracle” BCF run on just the 5 relevant predictors (oracle BCF-5) and Sparse BCF (SP-BCF-10), averaged over $H = 500$ Monte Carlo simulations. Performance of the methods is measured through: bias, defined as $\mathbb{E}[(\hat{\tau}_i - \tau_i) \mid \mathbf{X}_i = \mathbf{x}_i]$; the quadratic loss function

$$\mathbb{E}[(\hat{\tau}_i - \tau_i)^2 \mid \mathbf{X}_i = \mathbf{x}_i] , \quad (15)$$

where $\hat{\tau}_i$ is the model-specific CATE estimate, while τ_i is the ground-truth CATE; and finally 95% frequentist coverage, defined as $\mathbb{P}(\hat{\tau}(\mathbf{x}_i)_{\text{low}} \leq \tau(\mathbf{x}_i) \leq \hat{\tau}(\mathbf{x}_i)_{\text{upp}})$, where $\hat{\tau}(\mathbf{x}_i)_{\{\text{low}, \text{high}\}}$ are the upper and lower bounds of 95% credible interval around $\hat{\tau}(\mathbf{x}_i)$, returned by the MCMC. The loss function in (15) is also known as the *Precision in Estimating Heterogeneous Treatment Effects* (PEHE) from Hill (2011). Bias, PEHE and coverage estimates are estimated by computing, for each of the $H = 500$ Monte Carlo simulations, their sample equivalents

$$\widehat{\text{Bias}}_{\tau} = \frac{1}{N} \sum_{i=1}^N \left(\hat{\tau}(\mathbf{x}_i) - \tau(\mathbf{x}_i) \right)$$

$$\widehat{\text{PEHE}}_\tau = \frac{1}{N} \sum_{i=1}^N \left(\hat{\tau}(\mathbf{x}_i) - \tau(\mathbf{x}_i) \right)^2$$

$$\widehat{\text{Coverage}}_\tau = \frac{1}{N} \sum_{i=1}^N \mathbb{I} \left(\hat{\tau}(\mathbf{x}_i)_{low} \leq \tau(\mathbf{x}_i) \leq \hat{\tau}(\mathbf{x}_i)_{upp} \right) ,$$

and then averaging these over all the simulations. More precisely, Table 1 reports bias, $\sqrt{\text{PEHE}}$ and coverage estimates together with 95% Monte Carlo confidence intervals.

Sparse BCF shows better performance than default BCF and the “oracle” BCF version in terms of bias and $\sqrt{\text{PEHE}}$, while reports just marginally lower coverage, signalling that the method allocates “stick-breaking” splitting probabilities in an efficient way. This is because, even in the case where BCF explicitly knows which covariates to include a priori, it cannot adapt to different levels of smoothness for each covariate.

4.4 Targeted regularization in confounded studies

The parametrization in BCF, and thus in Sparse BCF as well, is designed to effectively disentangle prognostic and moderating effects of the covariates and to induce different levels of sparsity when estimating these effects, in contrast to other methods for CATE estimation. The purpose of this section is to briefly illustrate with a simple example how naively introducing sparsity through a model that does not explicitly guard against RIC can have a detrimental effect on CATE estimates. To this end, we simulate, for $N = 1000$ observations, $P = 5$ correlated covariates as $(X_1, \dots, X_5) \sim \mathcal{N}(\mathbf{0}, \Sigma)$, where the entries of the covariance matrix are $\Sigma_{jk} = 0.6^{|j-k|} + 0.1\mathbb{I}(j \neq k)$. The treatment allocation, prognostic score, CATE and response Y_i are then respectively generated as follows:

$$\begin{aligned} Z_i &\sim \text{Bernoulli}(\pi(\mathbf{x}_i)) , \\ \pi(\mathbf{x}_i) &= \Phi(-0.5 + 0.4X_{i,1}) , \\ \mu(\mathbf{X}_i) &= 3 + X_{i,1} , \\ \tau(\mathbf{X}_i) &= 0.5 + 0.5X_{i,2}^2 , \\ Y_i &= \mu(\mathbf{x}_i) + \tau(\mathbf{x}_i)Z_i + \varepsilon_i , \quad \text{where } \varepsilon_i \sim \mathcal{N}(0, 1) . \end{aligned} \tag{16}$$

Notice that in this simple setup the prognostic effect is determined by the first covariate $X_{i,1}$, while the moderating effect by the second covariate $X_{i,2}$. We run CATE estimation via three different methods that make use of sparse DART priors. The first is a “Single-Learner” (S-Learner) that employs DART (S-DART) to fit a single surface $f(\cdot)$ and computes CATE estimates as $\hat{\tau}(\mathbf{x}_i) = \hat{f}(\mathbf{x}_i, Z_i = 1) - \hat{f}(\mathbf{x}_i, Z_i = 0)$. The second is a “Two-Learner” (T-Learner) that employs DART (T-DART) to fit two separate surfaces, $f_1(\cdot)$ and $f_0(\cdot)$, for the two treatment groups and derives CATE estimates as $\hat{\tau}(\mathbf{x}_i) = \hat{f}_1(\mathbf{x}_i) - \hat{f}_0(\mathbf{x}_i)$. The last method is our Sparse BCF (SP-BCF). Each of these methods is able to account for sparsity when estimating CATE. However, the interpretation of variable importance is very different across them, due to the way the CATE estimator is derived. In particular, as indicated by

Table 2: Posterior splitting probabilities from S-Learner DART, T-Learner DART and Sparse BCF over the 5 available covariates. Values in bold denote which covariates receive significant chunks of splitting probability in fitting the corresponding functions, that characterize each model.

Method	$f(\cdot)$	Variable					
		X_1	X_2	X_3	X_4	X_5	Z
S-DART	$f(\cdot)$	0.12	0.43	0.00	0.00	0.00	0.45
T-DART	$f_0(\cdot)$	0.29	0.70	0.01	0.00	0.00	-
	$f_1(\cdot)$	0.09	0.90	0.00	0.01	0.00	-
SP-BCF	$\mu(\cdot)$	0.98	0.01	0.00	0.00	0.01	-
	$\tau(\cdot)$	0.00	0.96	0.00	0.03	0.01	-

the posterior splitting probabilities of each method in Table 2, S-DART fits a single surface $f(\cdot)$, where Z is treated as an extra covariate, so it ends up assigning most of the splitting probability to Z and then in turn to other relevant covariates. T-DART performs “group-specific” variable selection, in that it fits separate surfaces for each of the treatment groups. Although both S-DART and T-DART turn out to select the relevant covariates for the final estimation of CATE, they are unable, by construction, to attribute prognostic or moderating effects to each of them. Sparse BCF instead, thanks to its parametrization, is capable of doing so, disentangling the two effects.

In Section 5, we will show that Sparse BCF outperforms default BCF and other state-of-the-art methods in estimating CATE, through more challenging simulated exercises.

5 Simulated experiments

In this section, we provide results from two simulated studies carried out to demonstrate the performance of Sparse BCF and its informative prior version. The first simulated study is intended to evaluate Sparse BCF performance compared to other popular state-of-the-art methods for CATE estimation, and to show how it scales up with an increasing number of “nuisance” (irrelevant) covariates. In addition, we will also illustrate how the method implements variable selection by returning the computed posterior splitting probabilities on $\mu(\cdot)$ and $\tau(\cdot)$. The second simulated setup instead mimics a strongly confounded study, and is designed to show how versions of Sparse BCF deal with targeted selection scenarios. The R code implementing Sparse BCF is available at: <https://github.com/albicaron/SparseBCF>.

5.1 Comparison to other methods

The first fully simulated setup consists of two parallel simulated studies, with a different total number of predictors, $P = 25$ and $P = 50$ respectively, but everything else equal (same relevant predictors, same simulated surfaces, same sample size, etc.). The purpose underlying this setup is to illustrate how Sparse BCF relative performance scales up when nuisance predictors are added and the level of sparsity increases.

Table 3: List of models tested on the simulated experiment in Section 5.1.

Family	Label	Description
Linear Models	S-OLS	Linear regression as S-Learner
	T-OLS	Linear regression as T-Learner
	R-LASSO	LASSO regression as R-Learner
Naive Non-Parametrics	k NN	k -Nearest Neighbors as T-Learner
Tree-Based Methods	CF	Causal Forest
	S-BART	BART as S-Learner
	T-BART	BART as T-Learner
	BCF	Bayesian Causal Forest
	SP-BCF	Sparse Bayesian Causal Forest
Gaussian Processes	CMGP	Causal Multi-task Gaussian Process
	NSGP	Non-Stationary Gaussian Process

For both simulated exercises, sample size is set equal to $N = 1000$. In order to introduce correlation between the covariates, they are generated as correlated uniforms from a Gaussian Copula $C_{\Theta}^{\text{Gauss}}(u) = \Phi_{\Theta}(\Phi^{-1}(u_1), \dots, \Phi^{-1}(u_P))$, where Θ is a covariance matrix such that $\Theta_{jk} = 0.3^{|j-k|} + 0.1\mathbb{I}(j \neq k)$. A 40% fraction of the covariates is generated as continuous, drawn from a standard normal distribution $\mathcal{N}(0, 1)$, while the remaining 60% as binary, drawn from a binomial $\text{Bin}(N, 0.3)$. This translates into the first $P_{\text{num}} = 10$ covariates being continuous and the remaining $P_{\text{bin}} = 15$ being binary in the scenario where the total number of covariates is $P = P_{\text{num}} + P_{\text{bin}} = 25$; whilst, in the scenario where $P = P_{\text{num}} + P_{\text{bin}} = 50$, the first $P_{\text{num}} = 20$ are continuous and the remaining $P_{\text{bin}} = 30$ binary. Selection into treatment is described by:

$$\pi(\mathbf{x}_i) = \mathbb{P}(Z_i = 1 \mid \mathbf{X}_i = \mathbf{x}_i) = \Phi\left(-0.5 + 0.2X_{i,1} + 0.1X_{i,2} + 0.4X_{i,21} + \frac{\eta_i}{10}\right), \quad (17)$$

where $\Phi(\cdot)$ is the cumulative distribution function of a standard normal, and η_i is a noise component drawn from a uniform $\mathcal{U}(0, 1)$. The binary treatment assignment is then drawn as $Z_i \sim \text{Bernoulli}(\pi(\mathbf{x}_i))$. Prognostic score and CATE functions are simulated as follows:

$$\begin{aligned} \mu(\mathbf{x}_i) &= 3 + 1.5 \sin(\pi X_{i,1}) + 0.5(X_{i,2} - 0.5)^2 + 1.5(2 - |X_{i,3}|) + \\ &\quad + 1.5X_{i,4}(X_{i,21} + 1) \\ \tau(\mathbf{x}_i) &= 0.1 + |X_{i,1} - 1|(X_{i,21} + 2). \end{aligned} \quad (18)$$

Notice that only 5 predictors among $P \in \{25, 50\}$, namely $\{X_1, X_2, X_3, X_4, X_{21}\}$, are relevant to the estimation of the prognostic score and CATE. Eventually, the response variable Y_i is generated as:

$$Y_i = \mu(\mathbf{x}_i) + \tau(\mathbf{x}_i)Z_i + \varepsilon_i, \quad \text{where } \varepsilon_i \sim \mathcal{N}(0, \sigma^2). \quad (19)$$

The error term standard deviation is set equal to $\sigma = \frac{\hat{\sigma}_{\mu}}{2}$, where $\hat{\sigma}_{\mu}$ is the sample standard deviation of the simulated prognostic score $\mu(\mathbf{x}_i)$ in (18).

Table 4: Train and test set $\sqrt{\text{PEHE}}$ estimates, together with 95% confidence interval, in the case of $P = 25$ covariates and $P = 50$ covariates scenarios.

	$P = 25$		$P = 50$	
	Train	Test	Train	Test
S-OLS	1.91 ± 0.00	1.91 ± 0.01	1.91 ± 0.00	1.91 ± 0.01
T-OLS	1.41 ± 0.01	1.47 ± 0.01	1.68 ± 0.01	1.78 ± 0.01
R-LASSO	1.17 ± 0.01	1.19 ± 0.01	1.20 ± 0.01	1.22 ± 0.01
<i>k</i> NN	1.62 ± 0.01	1.66 ± 0.01	1.72 ± 0.01	1.76 ± 0.01
CF	1.05 ± 0.01	1.05 ± 0.01	1.23 ± 0.01	1.23 ± 0.01
S-BART	0.77 ± 0.01	0.79 ± 0.01	0.85 ± 0.01	0.86 ± 0.01
T-BART	1.11 ± 0.01	1.11 ± 0.01	1.28 ± 0.01	1.29 ± 0.01
BCF	0.79 ± 0.01	0.82 ± 0.01	0.86 ± 0.01	0.88 ± 0.01
SP-BCF	0.54 ± 0.01	0.56 ± 0.01	0.55 ± 0.01	0.55 ± 0.01
CMGP	0.59 ± 0.01	0.61 ± 0.01	0.85 ± 0.03	0.77 ± 0.02
NSGP	0.60 ± 0.01	0.62 ± 0.01	0.74 ± 0.03	0.75 ± 0.03

Performance evaluation of each method is carried out through $\sqrt{\text{PEHE}}$ estimates, reported together with 95% Monte Carlo confidence intervals. Data are randomly split in 70% train set, used to train the models, and 30% test set to evaluate the model on unseen data. $\sqrt{\text{PEHE}}$ estimates are reported both for train and test data.

The models evaluated on the simulated data are summarized in Table 3. We make use of the Meta-Learners terminology described in Künzel et al. (2017) and Caron et al. (2020). The first set of models includes a S-Learner and a T-Learner least squares regression (S-OLS and T-OLS), and a R-Learner (Nie and Wager, 2020) LASSO regression (R-LASSO). The second set consists just in a naive k -nearest neighbors (*k*NN) as a T-Learner. The third set includes the following popular tree ensembles methods: Causal Forest (CF) developed by Wager and Athey (2018); a S-Learner and a T-Learner versions of BART (S-BART and T-BART); Bayesian Causal Forest by Hahn et al. (2020) (BCF); and finally our method, Sparse Bayesian Causal Forest (SP-BCF). The last set includes two causal multitask versions of Gaussian Processes, with stationary (CMGP) and non-stationary (NSGP) kernels respectively, both implementing also Automatic Relevance Determination over the covariates to achieve sparsity (Alaa and van der Schaar, 2017, 2018).

Performance of each method, for the two simulated scenarios with $P = 25$ and $P = 50$ covariates respectively, is shown in Table 4. Results demonstrate high adaptability and scalability of Sparse BCF, as the method displays the lowest estimated error in both simulated scenarios, and its performance is not undermined when more nuisance covariates are added, while the other methods generally deteriorates.

Figure 1 shows how Sparse BCF correctly picks the relevant covariates behind both prognostic and moderating effects, in contrast to default BCF which assigns equal probability of being chosen as a splitting variable to each predictor. Notice also that results do not essentially vary between the $P = 25$ and the $P = 50$ scenarios (respectively first and second row

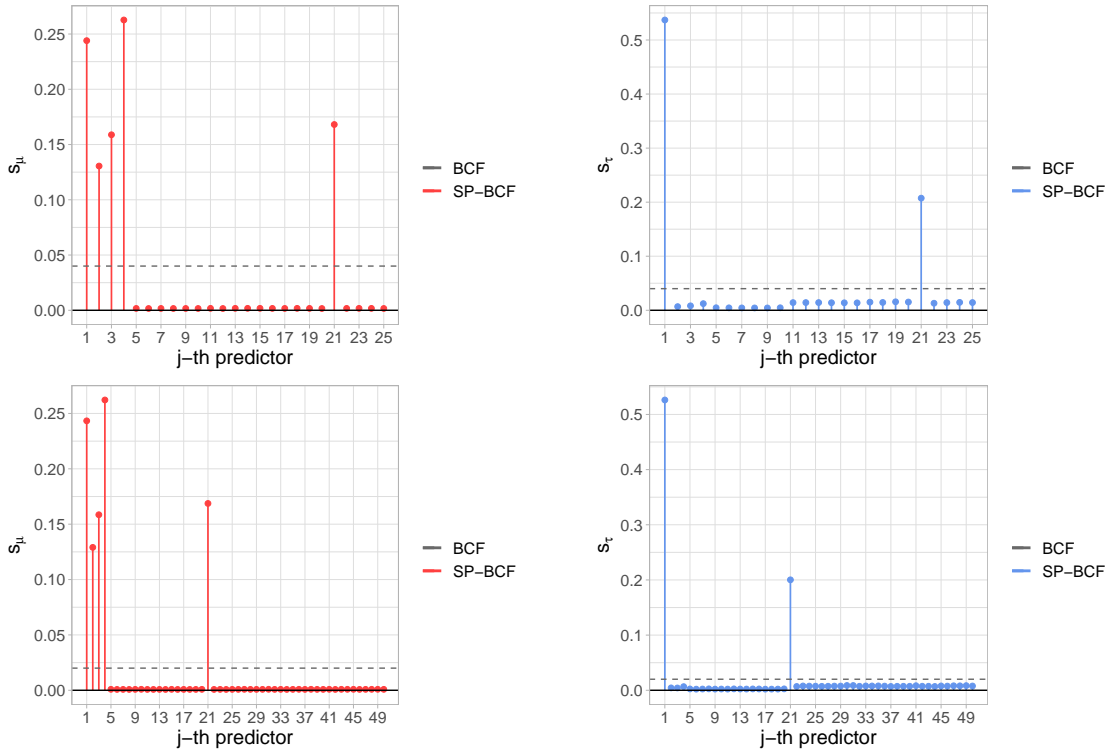


Figure 1: Sparse BCF posterior splitting probabilities for each single covariates, indexed on the x-axis, for $\mu(\cdot)$ (on the left) and $\tau(\cdot)$ (on the right), in the scenarios with $P = 25$ predictors (first row) and $P = 50$ predictors (second row). Spikes indicate higher probability assigned by Sparse BCF to the relevant predictors. The horizontal dashed lines denote default BCF uniform splitting probabilities.

graphs in Figure 1), as Sparse BCF virtually selects the same relevant predictors.

5.2 Strongly confounded simulated study

This section presents results from a second simulated study, aimed at showing how Sparse BCF addresses scenarios characterized by strong confounding. In particular, the setup is designed around the concept of targeted selection, a common type of selection bias in observational studies, expressively tackled by the BCF framework, that implies a direct relationship between $\mu(\cdot)$ and $\pi(\cdot)$. We run the simulated experiment in the usual way, by firstly estimating the unknown propensity score; then we also re-run the same experiment assuming that propensity score is known, to gain insights by netting out effects due to propensity model misspecification.

We simulate $N = 500$ observations from $P = 15$ correlated covariates (the first 5 continuous and the remaining 10 binary), generated as correlated uniforms from the Gaussian Copula $C_{\Theta}^{\text{Gauss}}(u) = \Phi_{\Theta}(\Phi^{-1}(u_1), \dots, \Phi^{-1}(u_P))$, where the covariance matrix is such that

Table 5: Bias, $\sqrt{\text{PEHE}}$, 95% Coverage and posterior splitting probability on $\hat{\pi}(x_i) — (s_\pi | u_\pi)$ — for: i) default BCF; ii) Sparse BCF; iii) Sparse BCF without $\hat{\pi}(x_i)$; iv) informative prior BCF with $k_{PS} = 50$; v) informative prior BCF with $k_{PS} = 100$.

Model	Bias	$\sqrt{\text{PEHE}}$	95% Coverage	$(s_\pi u_\pi)$
i) BCF	-0.06 ± 0.01	0.49 ± 0.01	0.94 ± 0.00	9.09%
ii) SP-BCF	-0.05 ± 0.01	0.38 ± 0.01	0.96 ± 0.00	0.29%
iii) SP-BCF (no PS)	-0.05 ± 0.01	0.38 ± 0.01	0.96 ± 0.00	-
iv) I-BCF ($k_{PS} = 50$)	-0.05 ± 0.01	0.39 ± 0.01	0.96 ± 0.00	9.76%
v) I-BCF ($k_{PS} = 100$)	-0.05 ± 0.01	0.40 ± 0.01	0.96 ± 0.01	17.48%

$\Theta_{jk} = 0.6^{|j-k|} + 0.1\mathbb{I}(j \neq k)$. The relevant quantities are simulated as follows:

$$\begin{aligned}
 \mu(\mathbf{x}_i) &= 5\left(2 + 0.5 \sin(\pi X_{i,1}) - 0.25 X_{i,2}^2 + 0.75 X_{i,3} X_{i,9}\right), \\
 \tau(\mathbf{x}_i) &= 1 + 2|X_{i,4}| + 1X_{i,10}, \\
 \pi(\mathbf{x}_i) &= 0.9 \Lambda(1.2 + 0.2\mu(\mathbf{x}_i)), \\
 Z_i &\sim \text{Bernoulli}(\pi(\mathbf{x}_i)), \\
 Y_i &= \mu(\mathbf{x}_i) + \tau(\mathbf{x}_i)Z_i + \varepsilon_i, \quad \text{where } \varepsilon_i \sim \mathcal{N}(0, \sigma^2),
 \end{aligned} \tag{20}$$

where $\Lambda(\cdot)$ is the logistic cumulative distribution function. The error's standard deviation is set equal to half the sample standard deviation of the generated $\tau(\cdot)$, $\sigma^2 = \frac{\hat{\sigma}_\tau}{2}$, and $\eta_i \sim \mathcal{U}(0, 1)$. Targeted selection is introduced by generating the propensity score $\pi(\mathbf{x}_i)$ as a function of the prognostic score $\mu(\mathbf{x}_i)$ (Hahn et al., 2020). The BCF models tested on this simulated setup are: i) Default BCF; ii) agnostic prior Sparse BCF; iii) agnostic prior Sparse BCF, without propensity score estimate as an additional covariate; iv) Sparse BCF with informative prior on $\mu(\cdot)$ only, where prior weight given to propensity score is $k_{PS} = 50$; v) Sparse BCF with the same prior as iv), but $k_{PS} = 100$. We test a variety of BCF versions to examine how they tackle confounding deriving from targeted selection. In particular, with iv) and v), we investigate whether nudging more splits on the propensity score covariate induces better handling of confounding and better CATE estimates. With ii) and iii) we study whether it is sensible to have propensity score as an extra covariate, once we have accounted for sparsity, in settings such as the one described in (20), where propensity $\pi(\cdot)$ and prognostic score $\mu(\cdot)$ are functions of the same set of covariates — more specifically $\pi(\cdot)$ is a function of $\mu(\cdot)$.

We first compare the usual performance metrics (bias, $\sqrt{\text{PEHE}}$, 95% coverage), averaged over $H = 500$ simulations, which are gathered in Table 5, together with the average posterior splitting probability assigned to propensity score $(s_\pi | u_\pi)$ by each model, where applicable. As for the posterior splitting probability $(s_\pi | u_\pi)$, we notice that in ii) this is nearly zero, thus not really different than not having $\pi(\cdot)$ at all, as in iii). This means that estimates of $\pi(\cdot)$ do not virtually contribute a lot to the fit. Also, in i) and iv), the probability is more or less the same, meaning that, in this example, setting $k_{PS} = 50$ implies assigning similar $(s_\pi | u_\pi)$ as default BCF, but allowing sparsity across the other covariates. In addition to the information in Table 5, for a better visual inspection, we plot the posterior fit of the $\pi(\cdot)$ and

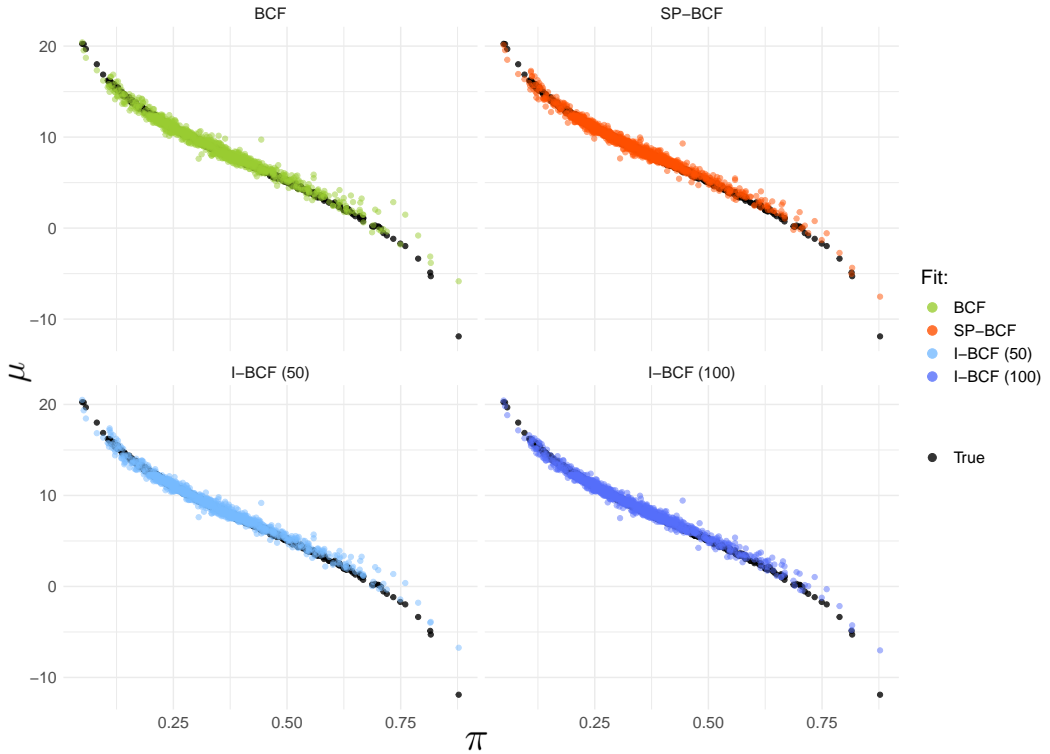


Figure 2: Posterior fit of $\pi(\cdot)$ and $\mu(\cdot)$ relationship, for default BCF, Sparse BCF (with $\pi(\cdot)$) and the two versions of informative prior BCF ($k_{PS} = 50$ and $k_{PS} = 100$). All the specifications effectively capture the underlying relationship.

$\mu(\cdot)$ relationship for each specification of BCF⁴.

The results corroborate those of the previous sections, as all the Sparse BCF versions ii)-v) outperform default BCF i), thanks to their ability to adapt to sparsity (Table 5). In order to net out effects that are due to propensity model misspecification, we re-run the same example in (20) for $H = 250$, this time assuming that PS is known, thus plugging in the true values in $\mu(\mathbf{x}_i, \pi)$. Results are displayed in Table 6 in the appendix.

The picture emerging from this exercise is the following. Methods ii)-v) all have comparable performances in the realistic scenario where PS is to be estimated (see Table 5); moreover, Figure 2 show that, in this case, they all effectively capture the relationship between $\pi(\cdot)$ and $\mu(\cdot)$. Hence, adjusting prior weights to nudge more splits on the estimated PS — methods iv) and v) — does not seem to improve performance. In the more abstract scenario where PS is assumed to be known (whose results are gathered in Table 6 in the appendix), and thus the relationship between $\pi(\cdot)$ and $\mu(\cdot)$ can be directly estimated, versions i) and iii) perform poorly. The first because it does not induce sparsity, while iii) does not include $\pi(\cdot)$ as extra covariate. Versions ii), iv) and v) instead perform comparatively better as they virtually as-

⁴We avoid plotting the fit for iii) Sparse BCF without $\pi(\cdot)$, since it yields very similar results to ii) Sparse BCF with $\pi(\cdot)$ — In Table 5, ii) allocates nearly 0% splits to $\pi(\cdot)$, as in iii).

sign all the splitting probability to $\pi(\cdot)$, leaving the other covariates out of the model. This is unsurprising in a setup where $\pi(\cdot)$ is known, as its relationship with $\mu(\cdot)$ is straightforwardly captured. Even under this abstract scenario, specifications iv) and v), which assign higher weight to $\pi(\cdot)$, do not show improvements on performance, as also the agnostic prior version ii) effectively allocates the entire splitting probability to the $\pi(\cdot)$ covariate.

Results from the example where PS is perfectly known are in line with the findings of Hahn et al. (2020) and shed light on why adding $\pi(\cdot)$ as an extra covariate is always helpful in tackling targeted selection. Naturally, the success of this practice in addressing strong confounding heavily depends on the quality of the approximation of $\pi(\cdot)$, that is, the quality of the propensity model that estimates $\hat{\pi}(\cdot)$.

6 Case study: the effects of early intervention on cognitive abilities in low birth weight infants

In this section, we illustrate the use of Sparse BCF by revisiting the study in Brooks-Gunn et al. (1992), which analyzes data from the Infant Health and Development Program (IHDP), found also in the more recent contribution of Hill (2011). The IHDP was a randomized controlled trial aimed at investigating the efficacy of educational and family support services, with pediatric follow-ups, in improving cognitive skills of low birth weight preterm infants, who are known to have developmental problems regarding visual-motor and receptive language skills (McCormick, 1985; McCormick et al., 1990). The study includes observations on 985 infants whose weight at birth was less than 2500 grams, across 8 different sites. About one third of the infants were randomly assigned to treatment ($Z_i = 1$), which consisted in routine pediatric follow-up (medical and developmental), in addition to frequent home visits to inform parents about child's progress and communicate instructions about recommended activities for the child. Following Hill (2011), the outcome variable (Y_i) we use is the score in a Stanford Binet IQ test, whose values can range from a minimum of 40 to a maximum of 160, taken at the end of the intervention period (child's age equal 3). The available final sample, obtained after removing 77 observations with missing IQ test score, consists of $N = 908$ data points, while the number of pre-treatment covariates amounts to $P = 31$. A full list of the variables included in the analysis, together with a short description, can be found in Table 7 in the appendix section.

Firstly, we estimate propensity score using a 1-hidden layer neural network classifier. Then we run Sparse BCF with default agnostic prior for 15 000 MCMC iterations in total, but we discard the first 10 000 as burn-in. As output, we obtain the full posterior distribution on CATE estimates and splitting probabilities relative to each covariate. The left-hand pane graph of Figure 3 shows the estimated CATE posterior distribution for the individuals in the sample whose estimated propensity corresponds, or is closest, to the i -th percentile of the estimated propensity distribution, where i is 0, 10, 20, ..., 100. The represented stratified CATE posterior distribution relative to these propensity values conveys information about the uncertainty around the estimates and depicts an overall positive and rather heterogeneous

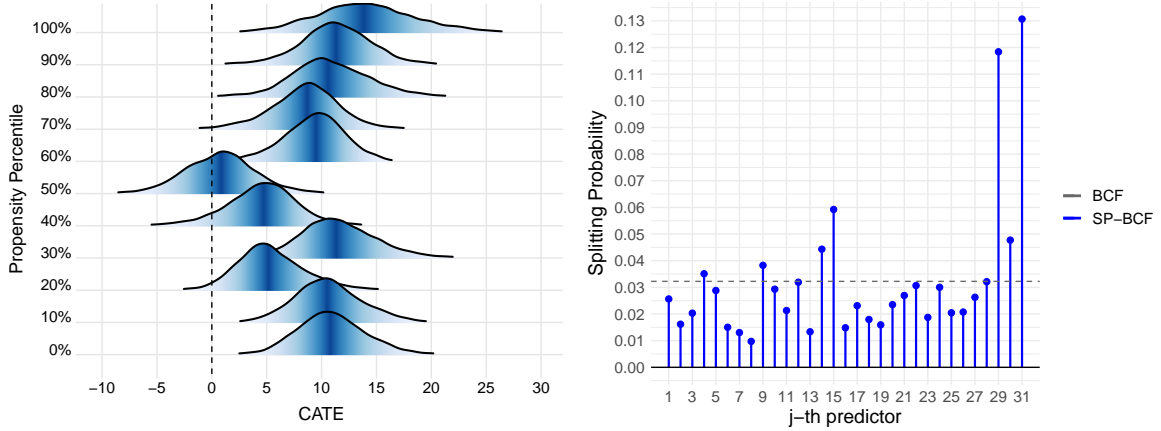


Figure 3: Left pane: Posterior distributions for the CATE estimates, obtained using Sparse BCF, corresponding to the approximated propensity percentiles (i.e. for individuals in the sample whose estimated propensity corresponds or is closest to the percentiles). Fill colour is darker around the median. Right pane: Sparse BCF’s posterior splitting probabilities on $\tau(\cdot)$, averaged over the post burn-in MCMC draws.

treatment effects. The estimated average treatment effect is equal to $\text{ATE} = 9.33$ and standard deviation of CATE estimates, averaged over the post burn-in draws, is equal to 3.25, which is another sign of underlying heterogeneity patterns in the treatment response. The analysis would thus benefit from further investigation about the heterogeneity of treatment effects, with the aim of distinguishing the impact within subgroups of individuals characterized by similar features (i.e. covariates values). Evidence on what the relevant drivers of heterogeneity behind treatment effect are is given by the posterior splitting probabilities on $\tau(\cdot)$ (again averaged over the post burn-in draws), reported in the right-hand pane graph of Figure 3, where few covariates end up being assigned relatively higher weights compared to the others. The two covariates that primarily stand out are the binary indicator on whether the mother’s ethnicity is white (29th predictor) and the ordinal variable indicating mother’s level of education (31st predictor).

We proceed with the analysis of subgroups by following the suggestion of Hahn et al. (2020), that is, we run a decision tree partition algorithm using the R package `rpart`, where average CATE estimates are treated as the target variable, while the covariates $X_i \in \mathcal{X}$ are used as predictors. The purpose of this exercise is to identify the most homogeneous subgroups in terms of their estimated CATE, and the covariates that lead to this optimal partition. Results are depicted in Figure 4 in the form of a decision tree, pruned at four levels. Zero splits trivially return ATE estimate (first node in Figure 4), while shallower nodes show CATE estimates averaged within the subgroup defined by the corresponding split rule. The first split is on the variable “Mother’s level of education”, specifically on whether the mother has attended college or not. The second level features a split on whether mother’s ethnicity is white in one branch, and a split on whether mother has finished high school in the other. These are exactly the same covariates selected by the posterior splitting probabilities.

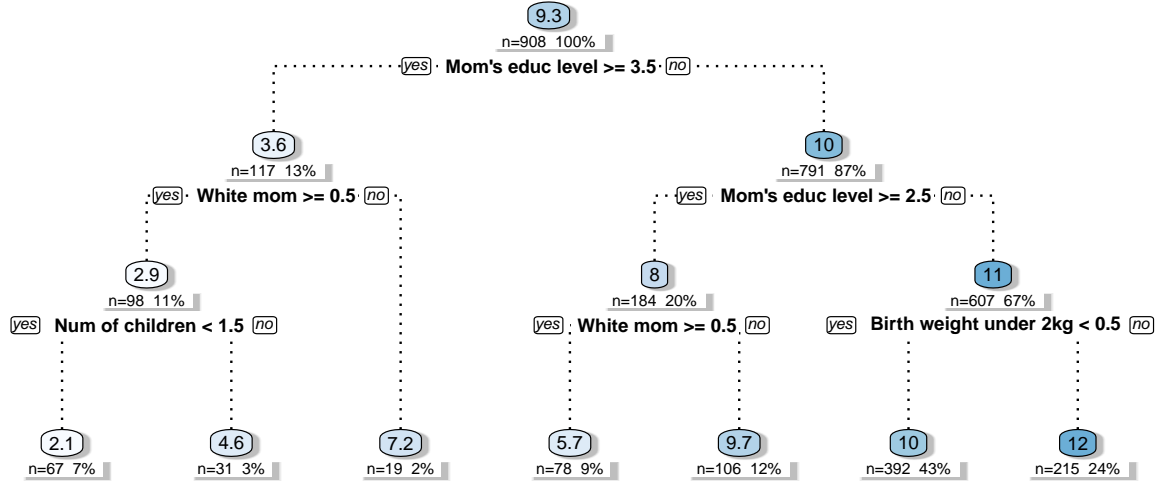


Figure 4: Decision tree identifying the most homogeneous subgroups in terms of treatment response, based on split rules involving the available covariates. The nodes report CATE estimates averaged within the corresponding subgroup.

The last set of splits is again on mother’s ethnicity, number of children the mother has given birth to and whether child’s birth weight is less than 2kg. Within these subgroups, CATE estimates range from a minimum of +2.1 to a maximum of +12.

Both CATE’s posterior splitting probabilities as well as subgroup analysis particularly point to covariates related to mother’s education and ethnicity, in addition to birth weight (in the subgroup analysis only). Results concerning heterogeneity stemming from mother’s ethnicity and child’s birth weight are consistent with those in the original (Brooks-Gunn et al., 1992) and follow-up studies Brooks-Gunn et al. (1994); McCarton et al. (1997), where the treatment effect is found to be lower for white mothers and for children with lower weight. The advantage of carrying out subgroup analysis through models such as Sparse BCF lies in the fact that subgroup identification can be done ex-post using CATE estimates, without the need of manually identifying the groups or partitioning the original sample ex-ante.

This illustrative example showed how Sparse BCF detects covariates which are responsible for the heterogeneity behind treatment impact in an example of real-world analysis, and how simple a posteriori partitioning of CATE estimates allows to derive optimal split rules to identify the most homogeneous subgroups in terms of treatment response. The analysis demonstrated that the estimation of individual (or subgroup) effects is a key factor for the correct evaluation and design of treatment administration policies.

7 Conclusion

In this work, we introduced a sparsity-inducing version of the popular nonparametric regression model Bayesian Causal Forest, recently developed by Hahn et al. (2020), in the context of heterogeneous treatment effects estimation. The new version proposed, which we refer to as Sparse Bayesian Causal Forest, is based on the contributions of Linero (2018) and Linero and Yang (2018), and differs in the two additional prior distributions that modify the way the model selects the covariates to split on. Sparse BCF allows variable selection to be carried out on the prognostic score and CATE surfaces separately, thus to account for sparsity, and by doing so delivers a more interpretable model a posteriori. In Section 5, we demonstrated its performance on simulated exercises that closely mimic confounded observational studies where only some of the covariates are relevant for the estimation, while the rest of them constitutes nuisance predictors and can cause bias if included in a fully-saturated model. Sparse BCF demonstrates very promising performance compared to the original version of BCF and to other state-of-the-art methods for CATE estimation, and also shows robustness to increasing number of nuisance covariates, while other methods generally tend to deteriorate. We also showed that it effectively tackles strong confounding in a simulated targeted selection scenario, a property inherited from the BCF parametrization. Finally, we illustrated its use in a real-world type of analysis.

Besides the implementation of variable selection per se, the additional advantage of Sparse BCF specification is that the pair of Dirichlet priors placed on the splitting probabilities can be tailored to incorporate subject-matter knowledge about the importance and impact of the covariates, separately for prognostic score and CATE estimation. Embedding of prior information in a Bayesian fashion represents a way of avoiding a completely agnostic model, that nonetheless benefits from the excellent predictive properties of a nonparametric regression algorithm such as BART. Hence, the informative version of Sparse BCF goes in the direction of a less “automated” method, which can be useful in applied studies with limited sample size, where a priori knowledge is possessed and can be efficiently incorporated without losing the benefits of using a powerful non-linear model.

References

- A. Alaa and M. van der Schaar. Limits of estimating heterogeneous treatment effects: Guidelines for practical algorithm design. In J. Dy and A. Krause, editors, *Proceedings of the 35th International Conference on Machine Learning*, volume 80 of *Proceedings of Machine Learning Research*, pages 129–138, Stockholm, Sweden, 10–15 Jul 2018. PMLR. URL <http://proceedings.mlr.press/v80/alaa18a.html>.
- A. M. Alaa and M. van der Schaar. Bayesian inference of individualized treatment effects using multi-task gaussian processes. *CoRR*, abs/1704.02801, 2017. URL <http://arxiv.org/abs/1704.02801>.
- J. Angrist and J.-S. Pischke. *Mostly Harmless Econometrics: An Empiricist’s Companion*.

Princeton University Press, 1 edition, 2009. URL <https://EconPapers.repec.org/RePEc:pup:pbooks:8769>.

J. D. Angrist, G. W. Imbens, and D. B. Rubin. Identification of causal effects using instrumental variables. *Journal of the American Statistical Association*, 91(434):444–455, 1996. doi: 10.1080/01621459.1996.10476902. URL <https://www.tandfonline.com/doi/abs/10.1080/01621459.1996.10476902>.

S. Athey and G. Imbens. Recursive partitioning for heterogeneous causal effects. *Proceedings of the National Academy of Sciences*, 113(27):7353–7360, 2016. ISSN 0027-8424. doi: 10.1073/pnas.1510489113. URL <https://www.pnas.org/content/113/27/7353>.

L. Breiman. Random forests. *Mach. Learn.*, 45(1):5–32, Oct. 2001. ISSN 0885-6125. doi: 10.1023/A:1010933404324. URL <https://doi.org/10.1023/A:1010933404324>.

J. Brooks-Gunn, F. ruey Liaw, and P. K. Klebanov. Effects of early intervention on cognitive function of low birth weight preterm infants. *The Journal of Pediatrics*, 120(3):350–359, 1992. ISSN 0022-3476. doi: [https://doi.org/10.1016/S0022-3476\(05\)80896-0](https://doi.org/10.1016/S0022-3476(05)80896-0). URL <https://www.sciencedirect.com/science/article/pii/S0022347605808960>.

J. Brooks-Gunn, C. McCarton, P. Casey, M. McCormick, C. Bauer, J. Bernbaum, J. Tyson, M. Swanson, F. Bennett, and D. Scott. Early intervention in low-birth-weight premature infants. results through age 5 years from the infant health and development program. *JAMA*, 272(16):1257–1262, October 1994. ISSN 0098-7484. doi: 10.1001/jama.1994.03520160041040. URL <https://doi.org/10.1001/jama.1994.03520160041040>.

A. Caron, I. Manolopoulou, and G. Baio. Estimating individual treatment effects using non-parametric regression models: a review. *arXiv:2009.06472*, 2020.

H. A. Chipman, E. I. George, and R. E. McCulloch. Bayesian CART model search. *Journal of the American Statistical Association*, 93(443):935–948, 1998. ISSN 01621459. URL <http://www.jstor.org/stable/2669832>.

H. A. Chipman, E. I. George, and R. E. McCulloch. BART: Bayesian additive regression trees. *Ann. Appl. Stat.*, 4(1):266–298, 03 2010. doi: 10.1214/09-AOAS285. URL <https://doi.org/10.1214/09-AOAS285>.

A. P. Dawid. Causal inference without counterfactuals. *Journal of the American Statistical Association*, 95(450):407–424, 2000. ISSN 01621459. URL <http://www.jstor.org/stable/2669377>.

A. P. Dawid. Statistical causality from a decision-theoretic perspective. *Annual Review of Statistics and Its Application*, 2(1):273–303, 2015. doi: 10.1146/annurev-statistics-010814-020105. URL <https://doi.org/10.1146/annurev-statistics-010814-020105>.

V. Dorie, J. Hill, U. Shalit, M. Scott, and D. Cervone. Automated versus do-it-yourself methods for causal inference: Lessons learned from a data analysis competition. *Statist. Sci.*, 34(1):43–68, 02 2019. doi: 10.1214/18-STS667. URL <https://doi.org/10.1214/18-STS667>.

J. C. Foster, J. m. G. Taylor, and S. J. Ruberg. Subgroup identification from randomized clinical trial data. *Statistics in medicine*, 30 24:2867–80, 2011.

D. P. Green and H. L. Kern. Modeling Heterogeneous Treatment Effects in Survey Experiments with Bayesian Additive Regression Trees. *Public Opinion Quarterly*, 76(3):491–511, 09 2012. ISSN 0033-362X. doi: 10.1093/poq/nfs036. URL <https://doi.org/10.1093/poq/nfs036>.

P. R. Hahn, C. M. Carvalho, D. Puelz, and J. He. Regularization and confounding in linear regression for treatment effect estimation. *Bayesian Anal.*, 13(1):163–182, 03 2018. doi: 10.1214/16-BA1044. URL <https://doi.org/10.1214/16-BA1044>.

P. R. Hahn, J. S. Murray, and C. M. Carvalho. Bayesian regression tree models for causal inference: Regularization, confounding, and heterogeneous effects. *Bayesian Anal.*, 2020. doi: 10.1214/19-BA1195. URL <https://doi.org/10.1214/19-BA1195>. Advance publication.

J. Hartford, G. Lewis, K. Leyton-Brown, and M. Taddy. Deep IV: A flexible approach for counterfactual prediction. In D. Precup and Y. W. Teh, editors, *Proceedings of the 34th International Conference on Machine Learning*, volume 70 of *Proceedings of Machine Learning Research*, pages 1414–1423, International Convention Centre, Sydney, Australia, 06–11 Aug 2017. PMLR. URL <http://proceedings.mlr.press/v70/hartford17a.html>.

T. Hastie, R. Tibshirani, and J. Friedman. *The Elements of Statistical Learning*. Springer Series in Statistics. Springer New York Inc., New York, NY, USA, 2001.

J. J. Heckman. Sample selection bias as a specification error. *Econometrica*, 47(1):153–161, 1979. ISSN 00129682, 14680262. URL <http://www.jstor.org/stable/1912352>.

J. L. Hill. Bayesian nonparametric modeling for causal inference. *Journal of Computational and Graphical Statistics*, 20(1):217–240, 2011. doi: 10.1198/jcgs.2010.08162. URL <https://doi.org/10.1198/jcgs.2010.08162>.

P. W. Holland. Statistics and causal inference. *Journal of the American Statistical Association*, 81(396):945–960, 1986. doi: 10.1080/01621459.1986.10478354. URL <https://www.tandfonline.com/doi/abs/10.1080/01621459.1986.10478354>.

G. W. Imbens. Nonparametric estimation of average treatment effects under exogeneity: A review. *The Review of Economics and Statistics*, 86(1):4–29, 2004. doi: 10.1162/003465304323023651. URL <https://doi.org/10.1162/003465304323023651>.

G. W. Imbens and D. B. Rubin. *Causal Inference for Statistics, Social, and Biomedical Sciences: An Introduction*. Cambridge University Press, 2015. doi: 10.1017/CBO9781139025751.

P. E. Jacob, L. M. Murray, C. C. Holmes, and C. P. Robert. Better together? statistical learning in models made of modules, 2017.

F. D. Johansson, U. Shalit, and D. Sontag. Learning representations for counterfactual inference. In *Proceedings of the 33rd International Conference on International Conference on Machine Learning - Volume 48*, ICML'16, page 3020–3029. JMLR.org, 2016.

G. King and R. Nielsen. Why propensity scores should not be used for matching. *Political Analysis*, 2019.

S. Künzel, J. Sekhon, P. Bickel, and B. Yu. Meta-learners for estimating heterogeneous treatment effects using machine learning. *Proceedings of the National Academy of Sciences*, 116, 06 2017. doi: 10.1073/pnas.1804597116.

A. R. Linero. Bayesian regression trees for high-dimensional prediction and variable selection. *Journal of the American Statistical Association*, 113(522):626–636, 2018. doi: 10.1080/01621459.2016.1264957. URL <https://doi.org/10.1080/01621459.2016.1264957>.

A. R. Linero and Y. Yang. Bayesian regression tree ensembles that adapt to smoothness and sparsity. *Journal of the Royal Statistical Society: Series B (Statistical Methodology)*, 80(5):1087–1110, 2018. doi: <https://doi.org/10.1111/rssb.12293>. URL <https://rss.onlinelibrary.wiley.com/doi/abs/10.1111/rssb.12293>.

M. Lu, S. Sadiq, D. J. Feaster, and H. Ishwaran. Estimating individual treatment effect in observational data using random forest methods. *Journal of Computational and Graphical Statistics*, 27(1):209–219, 2018. doi: 10.1080/10618600.2017.1356325.

C. McCarton, J. Brooks-Gunn, I. Wallace, C. Bauer, F. Bennett, J. Bernbaum, R. Broyles, P. Casey, M. McCormick, D. Scott, J. Tyson, J. Tonascia, and C. Meinert. Results at age 8 years of early intervention for low-birth-weight premature infants. the infant health and development program. *JAMA*, 277(2):126—132, January 1997. ISSN 0098-7484. doi: 10.1001/jama.1997.03540260040033. URL <https://doi.org/10.1001/jama.1997.03540260040033>.

M. McCormick. The contribution of low birth weight to infant mortality and childhood morbidity. *The New England journal of medicine*, 312(2):82—90, January 1985. ISSN 0028-4793. doi: 10.1056/nejm198501103120204. URL <https://doi.org/10.1056/NEJM198501103120204>.

M. C. McCormick, S. L. Gortmaker, and A. M. Sobol. Very low birth weight children: Behavior problems and school difficulty in a national sample. *The Journal of Pediatrics*, 117(5):687–693, 1990. ISSN 0022-3476. doi: [https://doi.org/10.1016/S0022-3476\(05\)83322-0](https://doi.org/10.1016/S0022-3476(05)83322-0). URL <https://www.sciencedirect.com/science/article/pii/S0022347605833220>.

T. P. Morris, I. R. White, and M. J. Crowther. Using simulation studies to evaluate statistical methods. *Statistics in Medicine*, 38(11):2074–2102, 2019. doi: 10.1002/sim.8086. URL <https://onlinelibrary.wiley.com/doi/abs/10.1002/sim.8086>.

X. Nie and S. Wager. Quasi-oracle estimation of heterogeneous treatment effects. *Biometrika*, 09 2020. ISSN 0006-3444. doi: 10.1093/biomet/asaa076. URL <https://doi.org/10.1093/biomet/asaa076>. asaa076.

J. Pearl. *Causality: Models, Reasoning and Inference*. Cambridge University Press, USA, 2nd edition, 2009a. ISBN 052189560X.

J. Pearl. Remarks on the method of propensity score. *Statistics in Medicine*, 28(9):1415–1416, 2009b. doi: <https://doi.org/10.1002/sim.3521>. URL <https://onlinelibrary.wiley.com/doi/abs/10.1002/sim.3521>.

J. Pearl. Theoretical impediments to machine learning with seven sparks from the causal revolution. *Proceedings of the Eleventh ACM International Conference on Web Search and Data Mining - WSDM '18*, 2018. doi: 10.1145/3159652.3176182. URL <http://dx.doi.org/10.1145/3159652.3176182>.

S. Powers, J. Qian, K. Jung, A. Schuler, N. H. Shah, T. Hastie, and R. Tibshirani. Some methods for heterogeneous treatment effect estimation in high dimensions. *Statistics in Medicine*, 37(11):1767–1787, 2018. doi: 10.1002/sim.7623. URL <https://onlinelibrary.wiley.com/doi/abs/10.1002/sim.7623>.

P. M. Robinson. Root-n-consistent semiparametric regression. *Econometrica*, 56(4):931–954, 1988. ISSN 00129682, 14680262. URL <http://www.jstor.org/stable/1912705>.

P. R. Rosenbaum and D. B. Rubin. The central role of the propensity score in observational studies for causal effects. *Biometrika*, 70(1):41–55, 04 1983. ISSN 0006-3444. doi: 10.1093/biomet/70.1.41. URL <https://doi.org/10.1093/biomet/70.1.41>.

D. B. Rubin. Bayesian inference for causal effects: The role of randomization. *Ann. Statist.*, 6(1):34–58, 01 1978. doi: 10.1214/aos/1176344064. URL <https://doi.org/10.1214/aos/1176344064>.

A. Schuler, M. Baiocchi, R. Tibshirani, and N. Shah. A comparison of methods for model selection when estimating individual treatment effects, 2018.

U. Shalit, F. D. Johansson, and D. Sontag. Estimating individual treatment effect: Generalization bounds and algorithms. In *Proceedings of the 34th International Conference on Machine Learning - Volume 70*, ICML'17, page 3076–3085. JMLR.org, 2017.

S. Sivaganesan, P. Müller, and B. Huang. Subgroup finding via bayesian additive regression trees. *Statistics in Medicine*, 36(15):2391–2403, 2017. doi: 10.1002/sim.7276. URL <https://onlinelibrary.wiley.com/doi/abs/10.1002/sim.7276>.

J. Starling, J. Murray, P. Lohr, A. Aiken, C. Carvalho, and J. Scott. Targeted smooth bayesian causal forests: An analysis of heterogeneous treatment effects for simultaneous versus interval medical abortion regimens over gestation, 05 2019.

S. Wager and S. Athey. Estimation and inference of heterogeneous treatment effects using random forests. *Journal of the American Statistical Association*, 113(523):1228–1242, 2018. doi: 10.1080/01621459.2017.1319839. URL <https://doi.org/10.1080/01621459.2017.1319839>.

L. Yao, S. Li, Y. Li, M. Huai, J. Gao, and A. Zhang. Representation learning for treatment effect estimation from observational data. In S. Bengio, H. Wallach, H. Larochelle, K. Grauman, N. Cesa-Bianchi, and R. Garnett, editors, *Advances in Neural Information Processing Systems 31*, pages 2633–2643. Curran Associates, Inc., 2018.

C. Zigler, K. Watts, R. Yeh, Y. Wang, B. Coull, and F. Dominici. Model feedback in bayesian propensity score estimation. *Biometrics*, 69, 02 2013. doi: 10.1111/j.1541-0420.2012.01830.x.

C. M. Zigler and F. Dominici. Uncertainty in propensity score estimation: Bayesian methods for variable selection and model-averaged causal effects. *Journal of the American Statistical Association*, 109(505):95–107, 2014. doi: 10.1080/01621459.2013.869498. URL <https://doi.org/10.1080/01621459.2013.869498>. PMID: 24696528.

A Perfectly known propensities example

Table 6 displays results obtained from Section 5.2 simulated exercise, where PS is assumed to be known and thus not estimated. Results are averaged over $H = 250$ simulations.

Table 6: Bias, $\sqrt{\text{PEHE}}$, 95% Coverage and posterior splitting probability on the true $\pi(x_i) — (s_\pi | u_\pi)$ — for: i) default BCF; ii) Sparse BCF; iii) Sparse BCF without the true $\pi(x_i)$; iv) informative prior BCF with $k_{PS} = 50$; v) informative prior BCF with $k_{PS} = 100$.

Model	Bias	$\sqrt{\text{PEHE}}$	95% Coverage	$(s_\pi u_\pi)$
i) BCF	-0.03 ± 0.01	0.38 ± 0.02	0.95 ± 0.00	9.1%
ii) SP-BCF	-0.02 ± 0.01	0.31 ± 0.02	0.97 ± 0.00	95.5%
iii) SP-BCF (no PS)	-0.06 ± 0.01	0.39 ± 0.02	0.96 ± 0.01	-
iv) I-BCF ($k_{PS} = 50$)	-0.02 ± 0.01	0.31 ± 0.02	0.97 ± 0.00	96.9%
v) I-BCF ($k_{PS} = 100$)	-0.02 ± 0.01	0.31 ± 0.02	0.97 ± 0.00	96.9%

B Variables included in the analysis

Table 7 here below provide a full list of variables used for the analysis in Section 6.

Table 7: Variables from the Infant Health and Development Program (IHDP)

Variable	Description	Type
<i>iq</i>	Score in IQ test (outcome Y)	Numeric
<i>treat</i>	Participation to the program (treatment Z)	Binary
<i>bw</i>	Child's weight at birth (in grams)	Numeric
<i>momage</i>	Mother's age	Numeric
<i>nnhealth</i>	Neo-natal health index	Numeric
<i>birth.o</i>	Child's order of birth	Numeric
<i>parity</i>	Number of children	Numer
<i>moreprem</i>	Number of children born prematurely	Numeric
<i>cigs</i>	Smoke during pregnancy	Numeric
<i>alcohol</i>	Drinks during pregnancy	Numeric
<i>ppvt.imp</i>	Mother's PPVT test result 1 year post birth	Numeric
<i>bw_2000</i>	Birth weight above/below 2kg	Binary
<i>female</i>	Child is a female	Binary
<i>mlt.birt</i>	Number of multiple births	Ordinal
<i>b.marry</i>	Marital status at birth	Binary
<i>livwho</i>	What family member lives with the child	Ordinal
<i>language</i>	Language spoken at home	Binary
<i>whenpren</i>	Trimester when prenatal care started	Ordinal
<i>drugs</i>	Drug use during pregnancy	Binary
<i>othstudy</i>	Participating in other studies at the same time	Binary

<i>site1</i>	Site number 1	Binary
:	:	:
<i>site8</i>	Site number 8	Binary
<i>momblack</i>	Mother's ethnicity black	Binary
<i>momhisp</i>	Mother's ethnicity hispanic	Binary
<i>momwhite</i>	Mother's ethnicity white	Binary
<i>workdur.imp</i>	Mother worked during pregnancy	Binary
<i>momed4F</i>	Mother's education level	Ordinal